Behavioral/Systems/Cognitive

Inhibition of Conditioned Stimulus Pathway Phosphoprotein 24 Expression Blocks the Reduction in A-Type Transient K^+ Current Produced by One-Trial *In Vitro* Conditioning of *Hermissenda*

Ebenezer N. Yamoah,[1] Snezana Levic,[1] John B. Redell,[2] and Terry Crow[3]

[1]Center for Neuroscience, Department of Otolaryngology, University of California, Davis, California 95616, and [2]Vivian L. Smith Center for Neurologic Research and [3]Department of Neurobiology and Anatomy, University of Texas Medical School, Houston, Texas 77225

Long-term intrinsic enhanced excitability is a characteristic of cellular plasticity and learning-dependent modifications in the activity of neural networks. The regulation of voltage-dependent K^+ channels by phosphorylation/dephosphorylation and their localization is proposed to be important in the control of cellular plasticity. One-trial conditioning in *Hermissenda* results in enhanced excitability in sensory neurons, type B photoreceptors, of the conditioned stimulus pathway. Conditioning also regulates the phosphorylation of conditioned stimulus pathway phosphoprotein 24 (Csp24), a cytoskeletal-related protein containing multiple β-thymosin-like domains. Recently, it was shown that the downregulation of Csp24 expression mediated by an antisense oligonucleotide blocked the development of enhanced excitability in identified type B photoreceptors after one-trial conditioning without affecting short-term excitability. Here, we show using whole-cell patch recordings that one-trial *in vitro* conditioning applied to isolated photoreceptors produces a significant reduction in the amplitude of the A-type transient K^+ current (I_A) detected 1.5–16 h after conditioning. One-trial conditioning produced a depolarized shift in the steady-state activation curve of I_A without altering the inactivation curve. The conditioning-dependent reduction in I_A was blocked by preincubation of the photoreceptors with *Csp* antisense oligonucleotide. These results provide an important link between Csp24, a cytoskeletal protein, and regulation of voltage-gated ion channels associated with intrinsic enhanced excitability underlying pavlovian conditioning.

Key words: Hermissenda; Csp24; one-trial pavlovian conditioning; β-thymosin repeat protein; intrinsic enhanced excitability; A-type K^+ current

Introduction

In addition to well documented changes in synaptic function associated with experience and learning, modifications of intrinsic cellular excitability are associated with a number of examples of associative learning such as pavlovian conditioning (Woody and Engel, 1972; Woody et al., 1976; Disterhoft et al., 1986; Moyer et al., 1996; Thompson et al., 1996) (for invertebrate review, see Sahley and Crow, 1998). The regulation of voltage-dependent K^+ channels and their localization have been proposed to play a critical role in the control of cellular excitability. Recently, activity-dependent changes in the localization, phosphorylation, and activation of K^+ channels in pyramidal neurons have been identified (Misonou et al., 2004). In addition, a potential role for components of the cytoskeleton has been proposed to contribute to the alterations in K^+ channel clustering in cultured pyramidal neurons (Surmeier and Foehring, 2004). The interaction between channels and an actin-binding protein was supported by studies showing that Kv4.2 current density is substantially larger in filamen$^+$ cells compared with filamen$^-$ cells (Petrecca et al., 2000). The cytoskeleton has been proposed to play a major role in both experience-dependent synaptic plasticity and modifications in dendritic spine morphology (for review, see Fifkova and Morales, 1992; Halpain, 2000; Matus, 2000; Bonhoeffer and Yuste, 2002). However, the contribution of spatial and temporal regulation of the actin cytoskeleton to intrinsic cellular excitability is primarily unknown.

In *Hermissenda*, one site of intrinsic excitability changes produced by pavlovian conditioning is neurons in the conditioned stimulus (CS) pathway (Crow and Alkon, 1980; Farley and Alkon, 1982; Alkon et al., 1985; Crow, 1985, 1988; Goh et al., 1985; Matzel et al., 1990; Frysztak and Crow, 1993, 1994, 1997; Gandhi and Matzel, 2000; Crow and Tian, 2003). In animals that exhibit intrinsic enhanced excitability, a cytoskeletal-related protein, the phosphorylation of which is regulated by conditioning, has been identified in components of the CS pathway (Crow and Xue-Bian, 2000, 2002). Conditioned stimulus pathway phosphoprotein 24 (Csp24) is a cytoskeletal-related protein containing

Received Dec. 23, 2004; revised April 5, 2005; accepted April 7, 2005.

This work was supported by National Institutes of Health Grant MH-40860 to T.C. and National Science Foundation Grant IBN-0317123 to E.N.Y. We thank Diana Parker for assistance with this manuscript.

Correspondence should be addressed to Terry Crow, Department of Neurobiology and Anatomy, University of Texas Health Sciences Center, 6431 Fannin, Houston, TX 77030. E-mail: terry.crow@uth.tmc.edu.

DOI:10.1523/JNEUROSCI.5256-04.2005

 0270-6474/05/254793-08$15.00/0

multiple actin-binding domains (Crow et al., 2003), homologous to other β-thymosin repeat proteins (Van Troys et al., 1999; Boquet et al., 2000; Hertzog et al., 2002, 2004; Paunola et al., 2002). The expression and phosphorylation of Csp24 is essential to intermediate-term memory formation after one-trial *in vitro* conditioning (Crow et al., 1999, 2003). We showed previously that blocking the expression of Csp24 with an antisense oligonucleotide inhibited the development of intermediate-term memory expressed in identified type B photoreceptors as measured by enhanced excitability (Crow et al., 2003). Here, we report that one-trial *in vitro* conditioning produced a significant reduction in the transient K^+ current (I_A) detected at 1.5, 3.5, and 16 h after conditioning in identified type B photoreceptors compared with control groups. In addition, conditioning produced a depolarized shift in the steady-state activation curve of I_A without affecting the inactivation curve. Incubation of isolated type B photoreceptors with the *Csp* antisense oligonucleotide before one-trial conditioning blocked the reduction in I_A produced by conditioning. These results show that a reduction in I_A contributes to intrinsic enhanced excitability accompanying one-trial conditioning and that the modification in the voltage-dependent activation of I_A is dependent on the expression of Csp24.

Materials and Methods

Photoreceptor isolation. Adult *Hermissenda crassicornis* were obtained from Sea Life Supply (Sand City, CA). Animals were fed scallops and held in modified 50 ml tubes maintained in a tank with recirculating artificial seawater (ASW) kept at 12–14°C on a 12 h light/dark cycle. Dissection protocols of the CNS were followed as described previously (Yamoah and Crow, 1994; Yamoah, 1997). The CNSs were dissected in ASW and allowed to stabilize at 4°C for 10 min. The isolated CNSs were then treated with an enzyme mixture consisting of 1 mg/ml protease XXIV (Sigma, St. Louis, MO) and 3 mg/ml dispase II (Boehringer Mannheim, Mannheim, Germany) in ASW. The enzyme reaction was inactivated and the digestion terminated by several buffer exchanges performed over 10–15 min with ASW containing 1% bovine serum albumin at 4°C. The photoreceptors were then excised from the CNS, and the transparent capsule around the photoreceptors was gently torn apart to expose the underlying cells. Type A and B photoreceptors were identified as described previously (Yamoah and Crow, 1994).

One-trial conditioning procedure. The one-trial conditioning procedure has been described previously (Crow and Forrester, 1986, 1991). After 12 min of dark adaptation, the conditioning trial consisted of one 5 min presentation of light (10^{-4} W/cm^2), the CS, paired simultaneously with the application of 5-HT to the isolated photoreceptor. The conditioning trial was followed by a wash with normal ASW and 12 min in the dark. The final concentration of 5-HT in ASW was 10^{-4} M. Unpaired control groups received the light CS (5 min) followed by a 5 min period in the dark before applying 5-HT (5 min) to the isolated photoreceptors in the dark. The 5-HT was washed out after the 5 min exposure, and the photoreceptors were maintained in the dark for an additional 12 min.

To examine the role of Csp24 in the modification of I_A in isolated type B cells produced by one-trial *in vitro* conditioning, Csp24 protein synthesis was inhibited by preincubation with an antisense oligonucleotide before conditioning. The specificity of the *Csp* antisense oligonucleotide treatment was demonstrated previously by the absence of an effect on Csp24 expression and the development of enhanced excitability after incubation with a scrambled oligonucleotide. In addition, treatment with the *Csp* antisense oligonucleotide did not significantly affect the synthesis of other proteins implicated in the conditioning of *Hermissenda* (Crow et al., 2003). Isolated photoreceptors were incubated for 18–20 h in 5 μM unmodified *Csp* antisense oligonucleotides 5′-GTGCAAGTCGACGGAAGGA-3′ or ASW. After the incubation, isolated photoreceptors received the one-trial *in vitro* conditioning procedure or unpaired *in vitro* control procedure. After one-trial conditioning, A-type K^+ currents were examined in isolated lateral type B cells at 1.5, 3.5, and 16 h after conditioning. Unpaired controls were examined at 3.5 h, a time in which short-term changes in excitability had decreased to control levels as established by current-clamp procedures (Crow and Siddiqi, 1997; Crow et al., 1999).

Solutions. All chemicals were obtained from Sigma unless indicated. ASW used for dissection and the CNS wash contained the following (in mM): 400 NaCl, 10 KCl, 10 $CaCl_2$, 50 $MgCl_2$, 15 HEPES. The isolated nervous system and photoreceptors were incubated in a solution containing the following (in mM): 360 NaCl, 5 KCl, 5 K-glutamate, 10 $CaCl_2$,

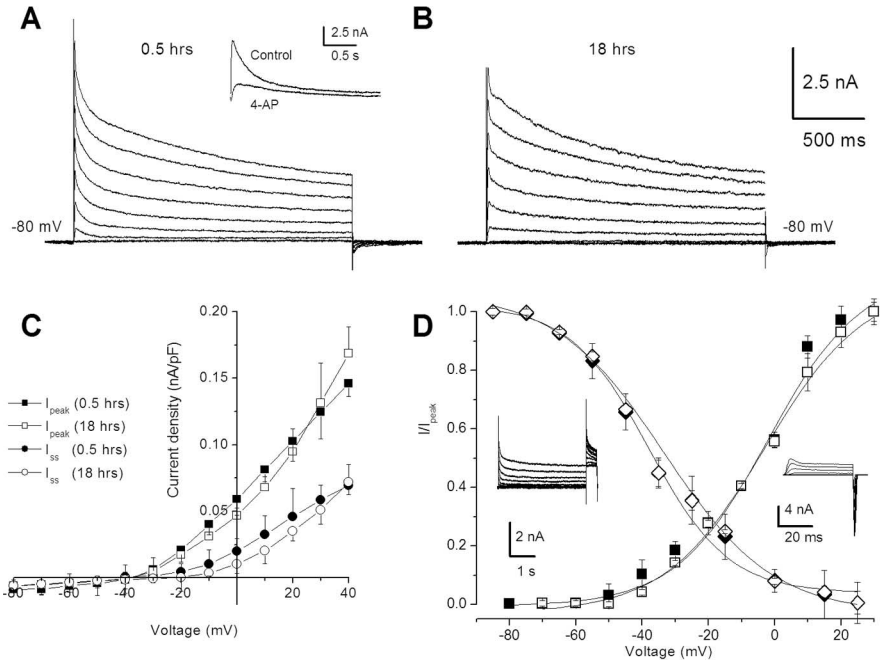

Figure 1. Whole-cell K^+ currents recorded from type B photoreceptors of *Hermissenda*. ***A***, Representative traces for a family of K^+ currents obtained from a holding potential of −80 mV and stepped up to +40 mV, with $\Delta V = 10$ mV. The recordings were made after 0.5 h in the incubation media. Inward sodium and calcium currents were reduced/removed by substituting choline for sodium and calcium ions. The duration of the stepped pulse in ***A*** and ***B*** was 2 s. Inset, The cell was held at −80 mV and then stepped to +30 mV for 2.5 s. The transient current was abolished by the application of 2.5 mM 4-AP. ***B***, Similar data obtained from a type B cell after 18 h of incubation. ***C***, Current density–voltage curve for peak and steady-state (I_{ss}) values obtained from type B cells (mean ± SD; $n = 9$). ***D***, Summary data of the steady-state activation and inactivation curves. The inset represents a typical steady-state inactivation protocol. The cell was held at −80 mV and stepped to a different prepulse for 4 s and then stepped to the +30 mV test pulse. The duration of the pulse shown in the inset for the deactivation current traces was 50 ms. Representative tail currents and current traces used to generate the curves are shown in the insets. For clarity, some of the current traces were not plotted. The activation and inactivation curves were obtained by plotting the normalized peak current (I/I_{peak}) at each test potential and then fitted by the following Boltzmann equations: $(I/I_{peak} = [1 + \exp(V_{1/2} - V)/k_m])^{-1}$ and $(I/I_{peak} = [1 + \exp(V - V_{1/2})/k_h])^{-1}$, respectively, where $V_{1/2}$ is the half-activation/inactivation voltage and $k_{m/h}$ is the maximum slope. The estimated $V_{1/2}$ and k_m from the activation curves were −2.7 ± 2.9 and 14.4 ± 2.3 mV (0.5 h; $n = 9$), 3.1 ± 1.8 mV, and 15.2 ± 1.0 mV (18 h; $n = 9$), respectively. For inactivation, the estimated $V_{1/2}$ and k_h from the inactivation curves were −33.3 ± 1.1 and 16.4 ± 0.94 mV (0.5 h; $n = 9$), −33.9 ± 2.01 mV, and 12.0 ± 4.2 mV (18 h; $n = 9$), respectively.

50 $MgCl_2$, 10 glucose, 15 HEPES. The solution was sterile-filtered, and the pH was adjusted to 7.8 with 1N NaOH. The extracellular or bath solution during recording of whole-cell K^+ currents consisted of the following (in mM): 360 choline chloride, 50 $MgCl_2$, 0.5 $CaCl_2$, 10 glucose, 100 KCl, 15 HEPES. This solution was sterile-filtered and adjusted to pH 7.7 with 1 M KOH. The external K^+ was increased to shift the reversal potential to approximately −35 mV, reduce the magnitude of the current, ensure adequate voltage control, and minimize the voltage-clamp error. The pipette solution contained the following (in mM): 400 KCl, 20 NaCl, 2 $MgCl_2$, 2 EGTA, 5 Na-ATP, 10 reduced glutathione, 50 HEPES. This was also sterile-filtered and adjusted to pH 7.4 with 1 M KOH. For all recording solutions, KCl was used to maintain an osmolarity of ~1000 mOsm.

Whole-cell K^+ current recordings. Whole-cell recordings were performed using standard patch-clamp recordings with an Axopatch 200B amplifier (Axon Instruments, Union City, CA). A horizontal electrode puller (model P-97; Sutter Instruments, Novato, CA) was used to make patch pipettes from borosilicate glass capillaries (outer diameter, 1.5 mm; inner diameter, 1 mm; World Precision Instruments, Sarasota, FL). Pipette tips were then fire-polished using a microforge (MF-830; Narishige, Tokyo, Japan) to obtain tip diameters ~1 μm. Using pipette solutions with an ionic strength equivalent to seawater (internal solution), the pipette resistances were ~0.8 MΩ, and only cells in experiments with seal resistances >1.2 GΩ were accepted for analysis. The access resistance was compensated by ~80%, and the estimated voltage error was ~4 mV given a maximum current of ~5 nA. A 3% agar bridge with 3 M KCl was used for the reference electrode. The membrane capacitances were measured using a brief pulse (10 ms) from a holding potential of −80 mV to a test potential of −100 mV. Statistically significant differences in capacitance between normal controls ($\bar{X}$ = 34.7 ± 5 pF) and one-trial *in vitro* conditioning ($\bar{X}$ = 26.8 ± 4.8 pF) were observed ($t_{(50)} = 5.8$; $p < 0.001$). Therefore, the current density of I_A was examined in conditioned and control groups. Currents were digitized through an analog-to-digital converter (Digidata 1200; Axon Instruments). Data collection was controlled through pClamp software (version 8.0; Axon Instruments), and experiments were performed at room temperature (~22°C). Data analysis of recorded currents was performed using Clampfit 8.1 (Axon Instruments) and Origin 6.0 (Microcal Software, Northampton, MA).

Statistical analysis. Descriptive statistics involved pooled data that were presented as means ± SD. Overall significant differences were examined with one-way ANOVA followed by *post hoc* two-group comparisons. In some comparisons, significant differences between two groups consisted of *t* tests for independent groups. A conservative α level ($p < 0.01$) was used with the ANOVA to establish overall significant differences.

Results

Whole-cell currents recorded at different times in the incubation media

Isolation and incubation of type B-photoreceptors do not adversely affect the elicitation of K^+ currents under the whole-cell voltage clamp. As shown in Figure 1, K^+ currents elicited from a holding potential of −80 mV and stepped to +40 mV were similar for photoreceptors incubated for 0.5 h (Fig. 1*A*) compared with 18 h (Fig. 1*B*). Group summary data shown in the current density–voltage curves in Figure 1*C* revealed similar values for peak and steady-state currents assessed at 0.5 and 18 h. The statistical analysis showed that there were no significant differences ($\bar{X}_D$ = 0.01) in the peak current measured at +20 mV for the 0.5 and 18 h groups ($t_{(16)} = 2.05$; NS). Significant differences in the steady-state current measured at +20 mV were not detected for the 0.5 and 18 h groups ($\bar{X}_D$ = 0.01) ($t_{(16)} = 1.89$; NS). The summary data for the steady-state activation and inactivation curves shown in Figure 1*D* were also similar for the 0.5 and 18 h groups. The mean ± SD of the half-activation voltage ($V_{1/2}$) at 0.5 h was −2.7 ± 2.9 mV and at 18 h, −3.1 ± 1.8 mV. The maximum slope (k_m) was 14.4 ± 2.3 mV at 0.5 h and 15.2 ± 1.0 mV for the 18 h group (Fig. 1*D*). The $V_{1/2}$ and k_h values for the inactivation curves were −33.3 ± 1.1 and 16.4 ± 0.94 mV for the 0.5 h group and −33.9 ± 2.01 and 12.0 ± 4.2 mV for the 18 h group. The insets of Figure 1*D* show representative tail currents and current traces used to generate the activation and inactivation curves. The time constants of activation and inactivation for the transient A-type K^+ current measured in type B photoreceptors was not changed after 18 h in the incubation medium (Fig. 2). The activation time constant of the transient component of the outward K^+ current measured at 0.5 h was virtually identical to the 18 h group (Fig. 2*A*). As shown in Figure 2*B*, the inactivation time constant of the transient outward K^+ current was not changed after 18 h in the incubation medium.

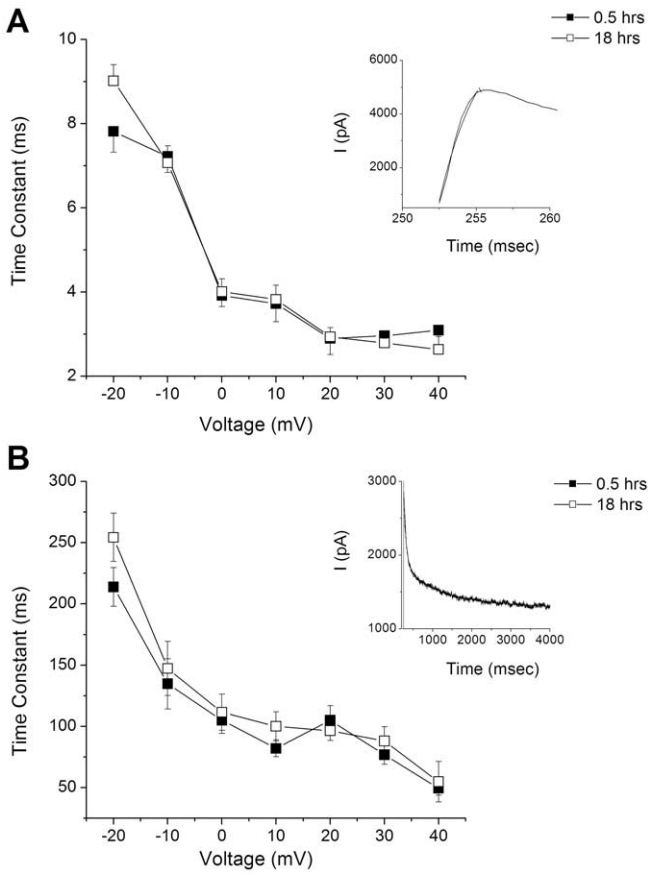

Figure 2. Time constants of activation and inactivation of I_A in B cells were unchanged after 18 h in the incubation media. ***A***, The activation time constant of I_A was fitted with a single-exponential function at different voltages for data collected at 0.5 and 18 h. The inset is an example of a trace used to generate the plot. ***B***, Similarly, the inactivation time constant remained unchanged after 18 h of incubation compared with 0.5 h in the incubation media. Error bars represent SD.

One-trial *in vitro* conditioning

One-trial conditioning produced a decrease in the current density of the transient A-type K^+ current in B photoreceptors measured from 1.5 to 16 h (Fig. 3). Representative current traces for the conditioned groups and normal controls are shown to the right in Figure 3*A*. The group summary data shown in the current density–voltage curve in Figure 3*A* revealed a decrease in current density for the conditioned groups ($n = 7$) relative to the control group ($n = 7$). The statistical analysis of differences measured at +20 mV showed an overall significant difference between the control and treatment groups ($F_{(3,28)} = 92.6$; $p < 0.001$). *Post hoc*

all pairwise multiple comparisons revealed that current densities for the 1.5 h group were significantly less than the control ($q = 14.4$; $p < 0.05$), the 3.5 h group was significantly reduced relative to the control group ($q = 19.3$; $p < 0.05$), and the 16 h group was significantly reduced relative to the controls ($q = 21.3$; $p < 0.05$). In addition, current densities for the 3.5 and 16 h groups were significantly less than the 1.5 h group ($q = 4.9$, $p < 0.05$; and $q = 6.9$, $p < 0.05$, respectively). In contrast, the unpaired control ($n = 6$) group shown in Figure 3*C* was not significantly different from the control ($n = 6$) with respect to the current density of the transient outward current ($t_{(10)} = 1.6$; NS). In addition, current densities of the unpaired control group ($\bar{X} = 0.13 \pm 0.005$) at 3.5 h were significantly different from the conditioned group ($\bar{X} = 0.06 \pm 0.01$) at 3.5 h ($t_{(12)} = 11.6$; $p < 0.01$). The steady-state activation curves of the transient A-type K^+ current in type B photoreceptors measured at 1.5, 3.5, and 16 h after conditioning revealed a depolarized shift compared with controls. With conditioning, $V_{1/2}$ was 24.7 ± 1.0, 19.5 ± 3.5, and 21.3 ± 2.6, and $V_{1/2} = 1.9 \pm 1.4$ for controls. However, the slopes were not significantly affected by conditioning. The maximum slopes were 15.9 ± 2.3, 14.2 ± 4.1, and 16.3 ± 1.8 for the conditioned groups and $k_m = 17.8 \pm 1.2$ for the controls (Fig. 3*B*).

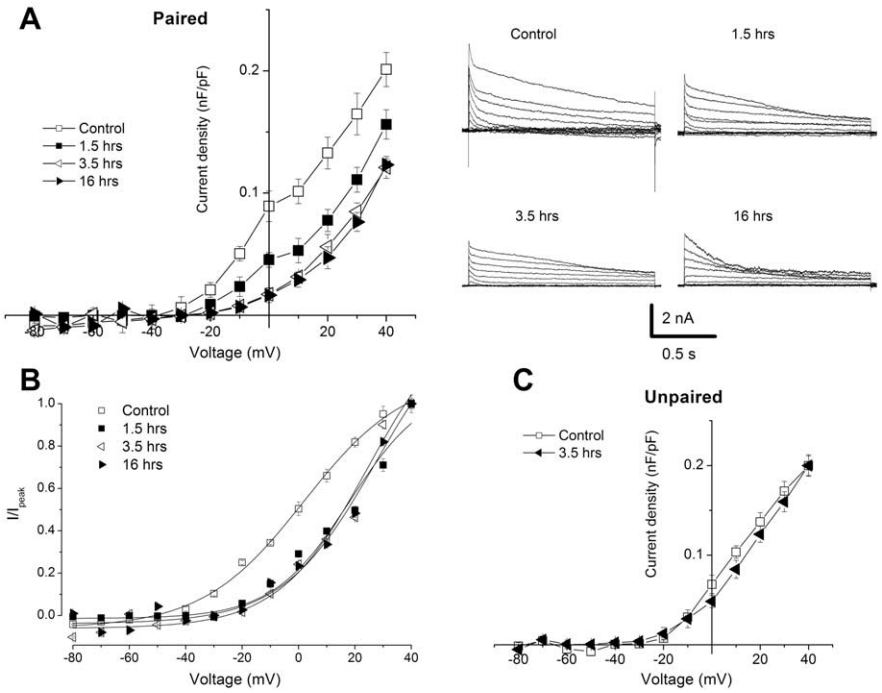

Figure 3. One-trial *in vitro* conditioning produced a significant reduction in the current density of I_A in B photoreceptors, which is reflected by alterations in the gating properties of the current. ***A***, Group summary data shown in current density–voltage plot of I_A for normal controls ($n = 8$) and conditioned groups measured 0.5 h ($n = 8$), 3.5 h ($n = 8$), and 16 h ($n = 8$) after conditioning. Representative current traces for the different groups are shown in the right panel. The duration of the stepped pulse was 1.5 s. ***B***, Steady-state activation of I_A in type B photoreceptors of *Hermissenda* measured at different times after one-trial conditioning. The activation curve was obtained by plotting the normalized peak I_A (I/I_{peak}) at each test potential and then fitted by the following Boltzmann equation: $(I/I_{peak} = [1 + \exp(V_{1/2} - V)/k_m])^{-1}$, where $V_{1/2}$ is the half-activation voltage, and k_m is the maximum slope. Overall significant differences were observed at different times for the conditioned groups compared with the control group ($p < 0.001$). ***C***, Summary group data shown in current density–voltage plot of I_A from normal controls ($n = 6$) and an unpaired group ($n = 6$) examined 3.5 h after the unpaired control procedure. In contrast to one-trial conditioning, there were no statistically significant differences between the normal control group and the unpaired control group at 3.5 h; however, the conditioned group at 3.5 h was significantly different from the unpaired control group ($p < 0.01$). Error bars represent SD.

One-trial *in vitro* conditioning reduced the steady-state activation of the transient K^+ conductance but did not alter the inactivation of the conductance. As shown in Figure 4*A*, the steady-state activation of the conductance at 1.5, 3.5, and 16 h was shifted to a more positive voltage compared with the control group. In contrast, the inactivation of the transient K^+ conductance was not affected by one-trial conditioning ($V_{1/2} = -34.1 \pm 2.5$, -32.3 ± 3.3, -36.1 ± 2.8 mV) compared with the controls ($V_{1/2} = -36.4 \pm 13$ mV) (Fig. 4*A*). An analysis of the steady-state properties of the A-type K^+ current revealed that one-trial conditioning produced an approximately threefold reduction in the transient current measured 1.5, 3.5, and 16 h after conditioning (Fig. 4*B*).

Antisense oligonucleotide treatment

Incubation of isolated type B photoreceptors with the antisense oligonucleotide blocked the reduction in the transient A-type K^+ current that is normally produced by one-trial conditioning. Examples of K^+ currents elicited from a holding potential of −80 mV and stepped to +40 mV with a ΔV of 10 mV are shown in Figure 5*A* for normal controls and in Figure 5*B* for antisense-treated groups. The transient outward K^+ currents were similar for both controls and antisense-incubated photoreceptors. The group summary data for the antisense controls and antisense-conditioned groups 1.5, 3.5, and 16 h after conditioning are shown in the current density–voltage curves in Figure 5*C*. The results of the ANOVA did not show a significant overall effect ($F_{(3,24)} = 3.6$; NS). These results show that blocking the expression of Csp24 by incubation of isolated type B photoreceptors with the Csp24 antisense oligonucleotide blocks the induction and development of the conditioning-dependent reduction in the transient A-type K^+ current.

The Csp24 antisense oligonucleotide incubation blocked the characteristic changes in the gating properties of the transient K^+ current produced by one-trial conditioning. As shown in Figure 6*A*, the steady-state activation and inactivation curves for the Csp24 antisense control groups were virtually identical to the antisense conditioned groups assessed 1.5, 3.5, and 16 h after conditioning. These results are in contrast to the effect of one-trial *in vitro* conditioning on the activation curves shown in Figure 4*A*. An examination of the steady-state properties of the current versus voltage revealed that the antisense oligonucleotide treatment blocked the change in the transient K^+ current as shown in Figure 6*B* for controls and groups tested 1.5, 3.5, and 16 h after conditioning.

Discussion

Previous studies of associative learning in *Hermissenda* have shown that pavlovian conditioning results in long-term intrinsic enhanced excitability of neurons in the CS pathway (Crow and Alkon, 1980; Farley and Alkon, 1982; West et al., 1982; Crow, 1985; Crow and Tian, 2003). Voltage-clamp studies identified a reduction in several K^+ currents, I_A and $I_{K,Ca}$, as contributors to conditioning-dependent enhanced excitability (Alkon et al.,

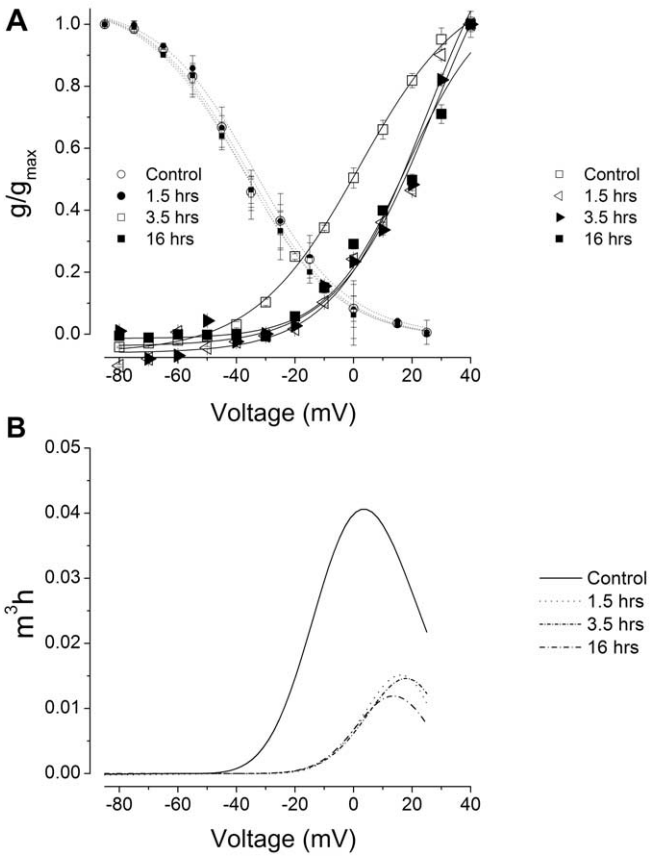

Figure 4. One-trial conditioning reduced (produced a rightward shift) the steady-state activation of I_A but did not alter the inactivation currents. ***A***, Steady-state activation and inactivation curves from the control group and groups tested 1.5, 3.5, and 16 h after one-trial conditioning. The conductances were estimated from the calculated reversal potential for K^+ (E_k, approximately −35 mV). In contrast to the activation curves, the inactivation curves were not shifted after conditioning. Thus, the magnitude and range of the window currents were reduced after conditioning. Error bars represent SD. g, Conductance; g_{max}, maximum conductance. ***B***, Assuming an m^3h state variable in the description of the steady-state properties of I_A, conditioning reduced the magnitude of I_A by approximately threefold. m^3, Activation state variable; h, inactivation state variable.

1982, 1985). Intrinsic enhanced excitability is a general mechanism of pavlovian conditioning as supported by studies of different examples of plasticity detected in several neural systems from diverse species (Woody and Engel, 1972; Woody et al., 1976; Disterhoft et al., 1986; Moyer et al., 1996; Thompson et al., 1996). In addition, enhanced local excitability of pyramidal neuron dendrites occurs with hippocampal long-term potentiation (LTP) (for review, see Johnston et al., 2003). The long-term modification of intrinsic enhanced excitability is proposed to be a function of alterations in voltage-gated ion channels. The local increase in dendritic excitability that accompanies LTP induction can be accounted for by a hyperpolarizing shift in the steady-state inactivation curve of I_A (Frick et al., 2004). Previously, pavlovian conditioning was shown to reduce the peak amplitude of I_A in type B photoreceptors of *Hermissenda* (Alkon et al., 1982). We have shown previously that one-trial conditioning results in intrinsic enhanced excitability of neurons in the CS pathway that is similar to modifications in excitability observed after multitrial conditioning (Crow and Forrester, 1991, 1993; Crow et al., 1996, 1999, 2003; Crow and Siddiqi, 1997). Potential changes in ion channel function underlying one-trial conditioning have not been examined, although simulation studies indicated that combinations of changes in voltage-dependent and Ca^{2+}-dependent conductances produced increases in 5-HT-dependent enhanced excitability comparable with experimental observations (Cai et al., 2003). Here, we have examined the contribution of I_A to enhanced excitability produced by one-trial conditioning.

In this report, we found that one-trial *in vitro* conditioning resulted in a shift in the activation of I_A to more depolarized potentials. The depolarizing shift in the activation curve for I_A was not accompanied by a significant change in the maximum slope of the activation curve at 1.5, 3.5, or 16 h after conditioning compared with controls. In addition, there were no significant changes in the inactivation curves for I_A assessed at different times after conditioning. We found that one-trial conditioning produced an approximately threefold reduction in I_A measured 1.5, 3.5, and 16 h after conditioning. Incubation of isolated identified type B photoreceptors with an antisense oligonucleotide directed at Csp24 blocked the reduction in I_A normally produced by one-trial conditioning. Blocking the expression of Csp24 by incubation of isolated type B photoreceptors with the *Csp* antisense oligonucleotide blocked the induction and development of the conditioning-dependent reduction in I_A. However, the antisense treatment did not affect the activation–inactivation curves for I_A at different times after conditioning compared with each postconditioning time and to normal controls (Fig. 6).

After the *in vitro* conditioning procedure, the current density of I_A plummeted in conditioned photoreceptors. Using the Hodgkin and Huxley (1952) formalism of whole-cell currents and the description of I_A in the photoreceptors by Sakakibara et al. (1993), the activation state variable m was reduced after conditioning, resulting in a profound reduction in the current magnitude (Fig. 4). The decline in the macroscopic tail current density observed in conditioned animals can reflect a reduction in single-channel amplitude, gating/open probability (p_o), or a decrease in the number of channels (N). Analyses of the steady-state activation of the whole-cell current, denoted by Np_o versus voltage, suggest that conditioning may alter one of the variables. Because the slope factor of the activation curves were essentially unaltered, it is unlikely that the gating kinetics of the channel is affected by conditioning. However, changes in the number of functional channels and a reduction in the single-channel conductance are a possible means by which I_A may be reduced. Therefore, the elementary properties of the channel must be assessed before a definitive conclusion can be reached.

In a previous study, we found that selective inhibition of Csp24 synthesis by incubation with an unmodified antisense oligonucleotide blocked the expression of intermediate-term enhanced excitability while leaving short-term enhanced excitability intact (Crow et al., 2003). The effect exhibited specificity, because other proteins implicated in conditioning-dependent plasticity in *Hermissenda* were not significantly affected by the antisense treatment. Moreover, incubation in a scrambled oligonucleotide did not reduce Csp24 synthesis or block enhanced excitability associated with intermediate-term memory (Crow et al., 2003).

How does a cytoskeletal-related protein such as Csp24 contribute to the modifications in ion channel function accompanying one-trial conditioning? The assembly and disassembly of actin filaments induced by extracellular signals contribute to a number of cellular processes. The actin cytoskeleton has been proposed to play a key role in cellular and synaptic plasticity (Fifkova and Morales, 1992; Matus, 2000; Kim and Lisman, 1999; Fischer et al., 2000; Halpain, 2000; Zhou et al., 2000). To perform functions supporting cellular plasticity, the organization of the

actin cytoskeleton requires both temporal and spatial regulation. The activity of these proteins is in turn modulated by intracellular signals, resulting in the recruitment of actin nucleation and polymerization at specific cellular sites (for review, see Schmidt and Hall, 1998). The synthesis and regulation of Csp24 by phosphorylation is a likely mechanism that could influence actin dynamics. Recent studies have shown that neuronal activity may alter the localization and properties of K^+ channels contributing to intrinsic excitability. In cultured rat hippocampal pyramidal cells, glutamate stimulation causes a dephosphorylation of Kv2.1 K^+ channels, a translocation of the channels from clusters to a more uniform distribution, and a shift in the activation curve for I_K (Misonou et al., 2004).

A major aspect of the contribution of actin to cellular plasticity may also involve its role in anchoring ion channels to the plasma membrane, in addition to directly contributing to the regulation of K^+ channel activity (Ehrhardt et al., 1996; Maguire et al., 1998; Maruoka et al., 2000). Interestingly, studies of inward rectifier channels have identified actin-binding proteins that may contribute to the anchoring and stabilization of ion channels in the plasma membrane (Leonoudakis et al., 2004). In addition, voltage-gated channels can interact with cytoplasmic proteins that may modulate channel function. The cytoplasmic scaffold protein filamin A contributes to the localization of cyclic nucleotide-gated cation pacemaker channels (Gravante et al., 2004). Filamin has been proposed to function as a scaffolding protein in the postsynaptic density that mediates a link between Kv4.2 channels and actin (Petrecca et al., 2000).

Previous work has shown that the enhanced excitability of type B photoreceptors is associated with 5-HT-dependent modulation of the sustained Ca^{2+} current, a hyperpolarization-activated inward rectifier current, and several K^+ conductances (I_A, $I_{K,Ca}$) (Acosta-Urquidi and Crow, 1993; Yamoah and Crow, 1995, 1996). Reductions in I_A shown here would be expected to enhance excitability. Therefore, the regulation of Csp24 by one-trial conditioning may contribute to changes in K^+ channel organization or distribution by influencing actin filament activity or affect channel function by regulating actin filament dynamics and scaffolding proteins in neurons of the CS pathway during the intermediate-term transition period between short- and long-term memory.

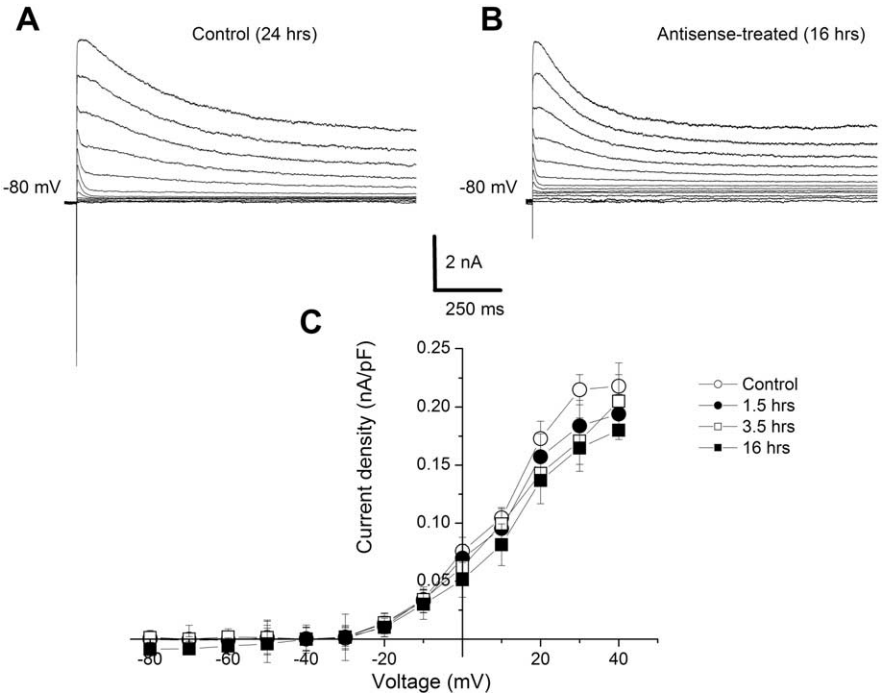

Figure 5. Csp antisense incubation blocked the reduction in I_A produced by one-trial conditioning. ***A***, Exemplary I_A current traces elicited from a holding potential of −80 mV to step potentials ranging from −80 to +40 mV with $\Delta V = 10$ mV. ***B***, Similar current traces elicited from an antisense-treated conditioned type B photoreceptor. ***C***, Group summary data in current density–voltage plot of I_A from the normal control group ($n = 7$) and groups examined 1.5 h ($n = 7$), 3.5 h ($n = 7$), and 16 h ($n = 7$) after one-trial conditioning. All conditioned groups were incubated in the antisense oligonucleotide. There were no statistically significant changes in the current densities in antisense-treated B cells measured at the different times after conditioning relative to the control group. Error bars represent SD.

References

Acosta-Urquidi J, Crow T (1993) Differential modulation of voltage-dependent currents in *Hermissenda* type B photoreceptors by serotonin. J Neurophysiol 70:541–548.

Alkon DL, Lederhendler I, Shoukimas JJ (1982) Primary changes of membrane currents during retention of associative learning. Science 215:693–695.

Alkon DL, Sakakibara M, Forman R, Harrigan J, Lederhendler I, Farley J (1985) Reduction of two voltage-dependent K^+ currents mediates retention of a learned association. Behav Neural Biol 44:278–300.

Bonhoeffer T, Yuste R (2002) Spine motility: phenomenology, mechanisms, and function. Neuron 35:1019–1027.

Boquet I, Boujemaa R, Carlier M-F, Preat T (2000) Ciboulot regulates actin assembly during *Drosophila* brain metamorphosis. Cell 102:797–808.

Cai Y, Baxter DA, Crow T (2003) Computational study of enhanced excitability in *Hermissenda*: membrane conductances modulated by 5-HT. J Comput Neurosci 15:105–121.

Crow T (1985) Conditioned modification of phototactic behavior in *Hermissenda.* II. Differential adaptation of B-photoreceptors. J Neurosci 5:215–223.

Crow T (1988) Cellular and molecular analysis of associative learning and memory in *Hermissenda.* Trends Neurosci 11:136–147.

Crow T, Alkon DL (1980) Associative behavioral modification in *Hermissenda*: cellular correlates. Science 209:412–414.

Crow T, Forrester J (1986) Light paired with serotonin mimics the effect of conditioning on phototactic behavior of *Hermissenda.* Proc Natl Acad Sci USA 83:7975–7978.

Crow T, Forrester J (1991) Light paired with serotonin *in vivo* produces both short- and long-term enhancement of generator potentials of identified B-photoreceptors in *Hermissenda.* J Neurosci 11:608–617.

Crow T, Forrester J (1993) Down-regulation of protein kinase C and kinase inhibitors dissociate short- and long-term enhancement produced by one-trial conditioning of *Hermissenda.* J Neurophysiol 69:636–641.

Crow T, Siddiqi V (1997) Time-dependent changes in excitability after one-trial conditioning of *Hermissenda.* J Neurophysiol 78:3460–3464.

Crow T, Tian L-M (2003) Neural correlates of Pavlovian conditioning in components of the neural network supporting ciliary locomotion in *Hermissenda.* Learn Mem 10:209–216.

Crow T, Xue-Bian JJ (2000) Identification of a 24 kDa phosphoprotein associated with an intermediate stage of memory in *Hermissenda.* J Neurosci 20:RC74(1–5).

Crow T, Xue-Bian JJ (2002) One-trial *in vitro* conditioning regulates a cytoskeletal-related protein (Csp24) in the conditioned stimulus pathway of *Hermissenda.* J Neurosci 22:10514–10518.

Crow T, Siddiqi V, Zhu Q, Neary JT (1996) Time-dependent increase in

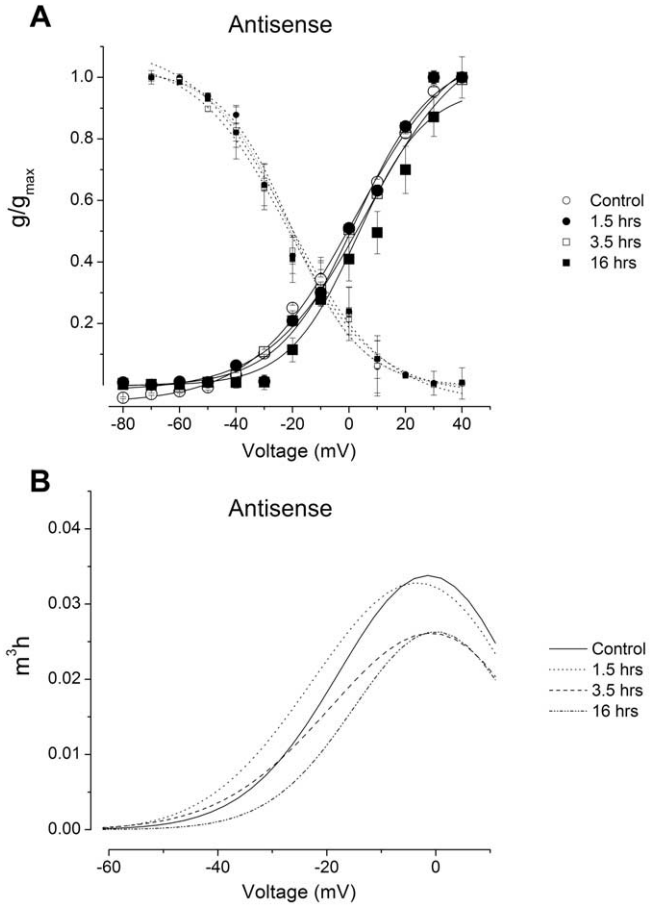

Figure 6. Csp antisense blocked the characteristic changes in the gating properties of I_A in type B photoreceptors. ***A***, Steady-state activation and inactivation curves for the *Csp* antisense-treated groups examined 1.5, 3.5, and 16 h after one-trial conditioning and normal controls. The conductances were estimated from the calculated reversal potential for K^+ (E_k, approximately −35 mV). Compared with the control group, the activation and inactivation curves remained unchanged in contrast to the effects of conditioning (Fig. 4). Thus, the magnitude and range of the window currents were unaltered after conditioning for the groups incubated in the antisense oligonucleotide. Error bars represent SD. g, Conductance; g_{max}, maximum conductance. ***B***, Assuming an m^3h state variable in the description of the steady-state properties of the current, the *Csp* antisense treatment blocked the reduction in the magnitude of I_A normally observed after one-trial conditioning. m^3, Activation state variable; h, inactivation state variable.

protein phosphorylation following one-trial enhancement in *Hermissenda.* J Neurochem 66:1736–1741.

Crow T, Xue-Bian JJ, Siddiqi V (1999) Protein synthesis-dependent and mRNA synthesis-independent intermediate phase of memory in *Hermissenda.* J Neurophysiol 82:495–500.

Crow T, Redell JB, Tian LM, Xue-Bian J, Dash PK (2003) Inhibition of conditioned stimulus pathway phosphoprotein 24 expression blocks the development of intermediate-term memory in *Hermissenda.* J Neurosci 23:3415–3422.

Disterhoft JF, Coulter DA, Alkon DL (1986) Conditioning-specific membrane changes of rabbit hippocampal neurons measured *in vitro.* Proc Natl Acad Sci USA 83:2733–2737.

Ehrhardt AG, Frankish N, Isenberg G (1996) A large-conductance K^+ channel that is inhibited by the cytoskeleton in the smooth muscle cell line DDT1 MF-2. J Physiol (Lond) 496:663–676.

Farley J, Alkon DL (1982) Associative neural and behavioral change in *Hermissenda*: consequences of nervous system orientation for light- and pairing-specificity. J Neurophysiol 48:785–807.

Fifkova E, Morales M (1992) Actin matrix of dendritic spines, synaptic plasticity, and long-term potentiation. Int Rev Cytol 139:267–307.

Fischer M, Kaech S, Wagner V, Brinkhaus H, Matus A (2000) Glutamate receptors regulate actin-based plasticity in dendritic spines. Nat Neurosci 3:887–894.

Frick A, Magee J, Johnston D (2004) LTP is accompanied by an enhanced local excitability of pyramidal neuron dendrites. Nat Neurosci 71:126–135.

Frysztak RJ, Crow T (1993) Differential expression of correlates of classical conditioning in identified medial and lateral type A photoreceptors of *Hermissenda.* J Neurosci 13:2889–2897.

Frysztak RJ, Crow T (1994) Enhancement of type B and A photoreceptor inhibitory synaptic connections in conditioned *Hermissenda.* J Neurosci 14:1245–1250.

Frysztak RJ, Crow T (1997) Synaptic enhancement and enhanced excitability in presynaptic and postsynaptic neurons in the conditioned stimulus pathway of *Hermissenda.* J Neurosci 17:4426–4433.

Gandhi CL, Matzel LD (2000) Modulation of presynaptic action potential kinetics underlies synaptic facilitation of type B photoreceptors after associative conditioning in *Hermissenda.* J Neurosci 20:2022–2035.

Goh Y, Lederhendler I, Alkon DL (1985) Input and output changes of an identified neural pathway are correlated with associative learning in *Hermissenda.* J Neurosci 5:536–543.

Gravante B, Barbuti A, Milanesi R, Zappi I, Viscomi C, DiFrancesco D (2004) Interaction of the pacemaker channel HCN1 with filamin A. J Biol Chem 43847–43853.

Halpain S (2000) Actin and the agile spine: how and why do dendritic spines dance? Trends Neurosci 23:141–146.

Hertzog M, Yarmola EG, Didry D, Bubb MP, Carlier M-F (2002) Control of actin dynamics by proteins made of β-thymosin repeats. J Biol Chem 277:14786–14792.

Hertzog M, Heijenoort CV, Didry D, Gaudier M, Coutant J, Gigant B, Didelot G, Préat T, Knossow M, Guittet E, Carlier M-F (2004) The β-thymosin/WH2 domain: structural basis for the switch from inhibition to promotion of actin assembly. Cell 117:611–623.

Hodgkin AL, Huxley AF (1952) A quantitative description of membrane current and its application to conduction and excitation in nerve. J Physiol (Lond) 117:500–599.

Johnston D, Christie BR, Frick A, Gray R, Hoffman DA, Schexnayder LK, Watanabe S, Yuan LL (2003) Active dendrites, potassium channels and synaptic plasticity. Philos Trans R Soc Lond B Biol Sci 358:667–674.

Kim C-H, Lisman J (1999) A role of actin filament in synaptic transmission and long-term potentiation. J Neurosci 19:4314–4324.

Leonoudakis D, Conti LR, Anderson S, Radeke CM, McGuire LMM, Adams ME, Froehner SC, Yates III JR (2004) Protein trafficking and anchoring complexes revealed by proteomic analysis of inward rectifier potassium channel (Kir2.x)-associated proteins. J Biol Chem 279:22331–22346.

Maguire G, Connaughton V, Prat AG, Jackson Jr GR, Cantiello HF (1998) Actin cytoskeleton regulates ion channel activity in retinal neurons. NeuroReport 9:665–670.

Maruoka ND, Steele DF, Au BP-Y, Dan P, Zhang X, Moore EDW, Fedida D (2000) α-Actinin-2 couples to cardiac Kv1.5 channels, regulating current density and channel localization in HEK cells. FEBS Lett 473:188–194.

Matus A (2000) Actin-based plasticity in dendritic spines. Science 290:754–758.

Matzel LD, Lederhendler II, Alkon DL (1990) Regulation of short-term associative memory by calcium-dependent protein kinase. J Neurosci 10:2300–2307.

Misonou H, Mohapatra DP, Park EW, Leung V, Zhen D, Misonou K, Anderson AE, Trimmer JS (2004) Regulation of ion channel localization and phosphorylation by neuronal activity. Nat Neurosci 7:711–718.

Moyer JR, Thompson LT, Disterhoft JF (1996) Trace eyeblink conditioning increases CA1 excitability in a transient and learning-specific manner. J Neurosci 16:5536–5546.

Paunola E, Mattila PK, Lappalainen P (2002) WH2 domain: a small, versatile adapter for actin monomers. FEBS Let 513:92–97.

Petrecca K, Miller DM, Shrier A (2000) Localization and enhanced current density of the Kv4.2 potassium channel by interaction with the actin-binding protein filamin. J Neurosci 20:8736–8744.

Sahley CL, Crow T (1998) Invertebrate learning: current perspectives. In: Learning and memory (Martinez Jr JL, Kesner RP, eds), pp 197–209. New York: Academic.

Sakakibara M, Ikeno H, Usui S, Collin C, Alkon DL (1993) Reconstruction of ionic currents in a molluscan photoreceptor. Biophys J 65:519–527.

Schmidt A, Hall MN (1998) Signaling to the actin cytoskeleton. Annu Rev Cell Dev Biol 14:305–338.

Surmeier DJ, Foehring R (2004) A mechanism for homeostatic plasticity. Nat Neurosci 7:691–692.

Thompson LT, Moyer JR, Disterhoft JF (1996) Transient changes in excitability of rabbit CA3 neurons with a time-course appropriate to support memory consolidation. J Neurophysiol 70:1210–1220.

Van Troys M, Vanderkerckhove J, Ampe C (1999) Structural modules in actin-binding proteins: towards a new classification. Biochim Biophys Acta 1448:323–348.

West A, Barnes ES, Alkon DL (1982) Primary changes of voltage responses during retention of associative learning. J Neurophysiol 48:1243–1255.

Woody CD, Engel Jr J (1972) Changes in unit activity and thresholds to electrical stimulation of coronal-pericruciate cortex of cat with classical conditioning of different facial movements. J Neurophysiol 35:230–241.

Woody CD, Knispel JD, Crow TJ, Black-Cleworth PA (1976) Activity and excitability to electrical current of cortical auditory receptive neurons of awake cats as affected by stimulus association. J Neurophysiol 39:1045–1061.

Yamoah EN (1997) Potassium currents in presynaptic hair cells of *Hermissenda.* Biophys J 72:193–203.

Yamoah EN, Crow T (1994) Two components of calcium currents in the soma of photoreceptors of *Hermissenda.* J Neurophysiol 72:1327–1336.

Yamoah EN, Crow T (1995) Evidence for a contribution of I_{Ca} to serotonergic modulation of I_{KCa} in *Hermissenda* photoreceptors. J Neurophysiol 74:1349–1354.

Yamoah EN, Crow T (1996) Protein kinase and G-protein regulation of Ca^{2+} currents in *Hermissenda* photoreceptors by 5-HT and GABA. J Neurosci 16:4799–4809.

Zhou Q, Xiao M-Y, Nicoll R (2000) Contribution of cytoskeleton to the internalization of AMPA receptors. Proc Natl Acad Sci USA 98:1261–1266.